Journal Pre-proof

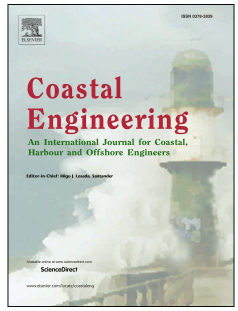

Cross-shore modelling of multiple nearshore bars at a decadal scale

B. Marinho, C. Coelho, M. Larson, H. Hanson

PII: S0378-3839(18)30495-2

DOI: https://doi.org/10.1016/j.coastaleng.2020.103722

Reference: CENG 103722

To appear in: *Coastal Engineering*

Received Date: 28 September 2018

Revised Date: 29 March 2020

Accepted Date: 2 May 2020

CROSS-SHORE MODELLING OF MULTIPLE NEARSHORE BARS AT A DECADAL SCALE

B. Marinho[1], C. Coelho[1], M. Larson[2], and H. Hanson[2]

[1] RISCO & Department of Civil Engineering, University of Aveiro, Aveiro, Portugal.
barbaramarinho@ua.pt; ccoelho@ua.pt

[2] Water Resources Engineering, Lund University, Lund, Sweden.
magnus.larson@tvrl.lth.se; hans.hanson@tvrl.lth.se

Abstract: This paper presents a numerical model designed to simulate subaqueous cross-shore profile behavior, including response of feeder mounds and barred systems. The present model development builds on the semi-empirical model proposed by Larson *et al.* (2013), designed to simulate the evolution of longshore bars exposed to incident waves, as well as the exchange of material between the bar and the berm region. Here, efforts are made to expand the theory for the evolution of a single-bar to a two-bar system, where the volumes of the individual bars (inner and outer) and their responses are modeled. In order to investigate the predictive capacity of the model, this exploratory numerical tool is first calibrated and validated against data from Duck, North Carolina, USA, where two bars typically appear (inner and outer). Field data derived from nearshore sand placement projects (Silver Strand State Park, California, and Cocoa Beach, Florida, USA), involving the construction of artificial longshore bars, are also employed to test the model in complex situations with diverse wave climates and typical beach profile shapes. The study presented in this paper shows that the equilibrium-based model is skilled at predicting the time-varying volume of the outer bar (ε=0.39; NMSE=0.24), suggesting that this morphological feature is strongly influenced by offshore wave forcing in a predictable, equilibrium-forced manner. Model skill was lower (ε=0.51; NMSE=0.29) when predicting the inner bar evolution at Duck, remaining questions about the predictability and the equilibrium-driven cross-shore behavior of more transient features. Model prediction of the evolution of feeder mounds (artificial bars) proved to be also successful through description of hypothetical bars characterized by zero equilibrium bar volume, leading to a good agreement with the field observations. Overall, the potential for using rather simple models to quantitatively reproduce the main trends of cross-shore volume changes in bars in a time perspective from years to decades has been demonstrated.

Keywords: subaqueous response, longshore bars, sediment transport, artificial nearshore placement, barred system, shoreline evolution, equilibrium state.

1. INTRODUCTION

Many wave dominated sandy coastal systems across the world are characterized by the presence of one or more subtidal longshore bars (Larson and Kraus, 1992; Ruessink and Kroon, 1994; Ruessink *et al.*, 2007; Walstra *et al.*, 2012; Van Enckevort and Ruessink, 2003; Różyński and Lin, 2015; Walstra *et al.*, 2015; Ruggiero *et al.*, 2016; Bouvier *et al.*, 2017; Aleman *et al.*, 2017; Stwart *et al.*, 2017; Eichentopf *et al.*, 2019). For such systems, models are required for simulating the bar-berm material exchange to reproduce: 1) the seasonal behavior of the beach profile; 2) the effects of the sediment release during storms from the dune and the beach to the subaqueous portion of the profile; and 3) the recovery process of the berm during periods of low-energy, when bars tend to lose volume and migrate onshore (eventually welding to the shore).

In support of coastal engineering and management activities, during the last few decades, a strong demand for sophisticated, robust, and reliable models for simulating coastal evolution over decades to centuries has emerged. The earliest type of long-term coastal evolution models focused on predicting the shoreline evolution in response to the potential sediment transport gradient generated by incident wave energy, following the one-line theory. According to this theory, firstly introduced by Pelnard-Considère (1956) and numerically implemented by numerous authors since then, beach profile moves parallel to itself, maintaining an equilibrium configuration. Thus, one-contour line can be used to describe changes in the beach shape and volume during accretionary and erosional events. Some examples of such models are GENESIS (Hanson, 1988), Unibest CL+ (Deltares, 2011), LITLINE in LITPACK (DHI, 2009a; 2009b, 2017) by DHI (Danish Hydraulic Institute) and LTC (Coelho, 2005). Although, these models can be used at large temporal (annual-decadal) and spatial scales (kilometers), one of their weaknesses has been the simplified representation of the cross-shore (CS) material exchange, where usually CS processes are incorporated through sink or source terms with representative values in time and space.

Profile evolution models, on the other hand, are commonly used to simulate the beach change on a short-term basis (hours to days), for investigating the impact of individual storms in the beach-dune system evolution, as well as the response of beach fills under storm conditions, *e.g.*, SBEACH (Larson and Kraus, 1989), LITPACK (LITPROF)

(DHI, 2008), XBEACH (Roelvink *et al.*, 2009), but also on a short- to medium-term (month to year) like Unibest TC by Deltares (Ruessink *et al.,* 2007; Walstra *et al.*, 2012). Nearshore morphology models simulating storm-induced changes have been widely applied for the last decade and demonstrated an acceptable level of accuracy as a result of well-defined cross-shore sediment transport equations, established numerical solutions, and high-quality field and laboratory data (Smith *et al.*, 2017).

Larson *et al.* (2013) developed a semi-empirical model to simulate the long-term response of longshore bars to incident wave conditions as well as the material exchange between the berm and bar region, through physics-based formulations and simple schematizations of the governing processes. Wijnberg and Kroon (2002) stated that long-term bar behavior results from many storm-recovery sequences and to arrive at these large scales, the integrated effect of short-term storm recovery sequences needs to be considered. Later, Larson *et al.* (2016) combined this model with modules to calculate dune erosion, overwash, and wind-blown sand (forming a unique-coupled system), in order to simulate the evolution of a schematized profile at a decadal scale.

Following the modelling approach proposed by Larson *et al.* (2013) and Larson et al. (2016), in this study, efforts are made to expand the theory of the evolution of one single bar to a multi-bar system, where the volume of the individual bars and their response are described, but without regard to the details of the profile/bar shape or how the material may be deposited in or removed from the surf zone. As a first step, a two-bar model is developed and validated with field data from Duck, North Carolina, where two bars (inner and outer) frequently form. The present model was also employed to numerically solve the evolution of offshore mounds through equilibrium equations as they migrate towards the shore and become a part of the beach face. The model was applied to simulate nearshore sand placements at Silver Strand, CA, and Cocoa Beach, FL, where in the latter case natural subtidal bars were not found.

The main objective of the present study is to enhance and validate a numerical approach developed in an equilibrium fashion to predict the subaqueous cross-shore beach profile response, including feeder mounds and multi-barred systems for applications in coastal evolution models, describing processes at the decadal scale. This paper is structured as follows. First, a brief review about the semi-empirical model proposed by Larson *et al.* (2013) is given, as this form the basis for the theoretical developments of the two-bar model described in section 2. Selected cases studies are addressed in section 3 through model application and discussion of the numerical results. Final conclusions are drawn in section 4.

2. MODEL DESCRIPTION

2.1. Theory for one bar and evolution equation

A subaqueous model developed to simulate bar-berm material exchange is briefly reviewed in this section, since a comprehensive description about the theoretical development is given in Larson *et al.* (2013, 2016) and Marinho *et al.* (2017b).

The proposed model assumes that the exchange of material between the bar and the berm takes place under sediment volume conservation, which means that no material is lost offshore. Material needed to supply the bar is mainly taken from the region of the inner surf zone, resulting in erosion of the subaerial beach. This process keeps taking place until a stable beach profile is achieved which dissipates wave energy without significant changes in shape. To reproduce this mechanism the volume eroded from the berm is available for the offshore bar (or, its representative morphological volume) that will tend to equilibrium (V_B=V_{BE}), if the wave conditions are steady and the sediment grain size does not vary (Larson *et al.*, 2013). However, cross-shore profiles are in constant change, *i.e.*, in dynamic equilibrium, with different time scales of morphological responses. So, in the model if the bar volume (V_B) at any given time is smaller than V_{BE}, then the bar volume will grow, whereas the opposite (V_{BE} < V_B) implies a decay in the bar volume. Figure 1 illustrates the cross-shore exchange of material between the subaqueous (bar) and subaerial (berm) portion of the profile.

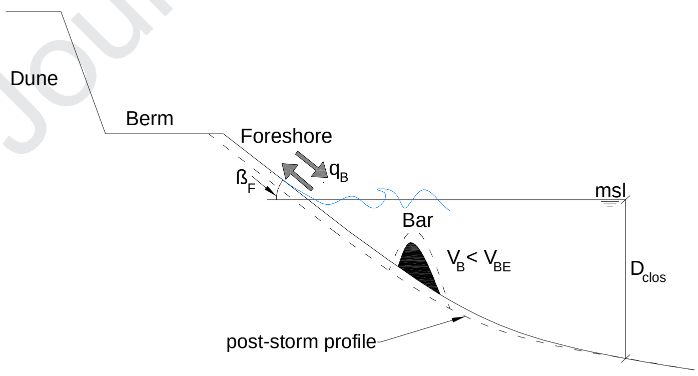

Figure 1. One-bar theory. The variables q_B, β_F, and D_{clos} denote the subaqueous transport rate between the bar and berm, foreshore slope, and depth-of-closure, respectively.

The change in bar volume per longshore unit (m^3/m) is taken to be proportional to the deviation from its equilibrium value,

$$\frac{dV_B}{dt}=\lambda(V_{BE}-V_B) \tag{1}$$

in which λ is a coefficient quantifying the rate at which equilibrium is approached. This coefficient depends on the sediment grain size (or fall speed, w), wave height at deep waters (H_0), wave period (T), and the λ_0 and m coefficients, which should be calibrated against data, according to:

$$\lambda=\lambda_0\left(\frac{H_0}{wT}\right)^m \quad (2)$$

A representative beach slope is implicitly contained in the fall speed (or grain size) because the equilibrium beach profile depends on this quantity (Dean, 1987). Observations of bar response to storms (*cf.*, Larson *et al.*, 2016) indicate that bars would exhibit a relatively larger growth in the field during energetic wave conditions, whereas the recovery process would be slower (during periods of calmer waves). An additional factor is used to adjust the coefficient λ_0 ($\lambda_0^{on}= C_c^{on}\lambda_0$; $\lambda_0^{off}= C_c^{off}\lambda_0$) when onshore or offshore sediment transport occurs ($V_{BE}<V_B$ and $V_{BE}>V_B$, respectively) as a way to better reproduce the observed bar behavior in the field, defined by a relatively slower response during onshore sediment-transport driving mechanisms (Larson *et al.*, 2016). Larson *et al.* (2016) suggested suitable values for m (=-0.5) and for λ_0 ($0.15h^{-1}$ and $0.002h^{-1}$, when applying Eq. 2 to laboratory and field data, respectively). Qualitatively, a larger value of λ produces a rapid response toward equilibrium. As bar position and depth are not explicit in the model, this parameter is a key parameter when quantifying the degree of disequilibrium term to express the time-varying position of the shoreline and sandbars. This was also found by by Davidson *et al.* (2013) and Splinter *et al.* (2018).

In order to apply Eq. 1, the equilibrium bar volume (V_{BE}) also needs to be determined. Larson and Kraus (1989) developed an empirically based expression for V_{BE}, based on large wave tank (LWT) experiments, where the normalized equilibrium bar volume was shown to depend on the dimensionless fall speed ($\Omega=H_0/w/T$) and the deep-water wave steepness (H_0/L_0),

$$\frac{V_{BE}}{L_0^2}=C_B\left(\frac{H_0}{wT}\right)^{4/3}\frac{H_0}{L_0} \quad (3)$$

in which L_0 is the deep-water wavelength and C_B is a dimensionless coefficient. According to Eq. 3, a larger wave height implies a larger bar volume and a greater fall speed (or larger grain size) implies a smaller bar volume (Larson and Kraus, 1989). For more information about the correlation and regression analysis detailing the degree of dependencies between variables consult Larson and Kraus (1989).

Considering changing wave input, Eq.1 has to be solved numerically, so, for each time step, Δt, the following analytical solution is employed,

$$V_B(t)=V_{BE}+(V_{B0}-V_{BE})e^{-\lambda t} \quad (4)$$

where V_{B0} is the bar volume at t=0. The bar volume changes equation (Eq.1) is applied during the growth and decay process of the bar, so, if $V_{BE}>V_{B0}$ the bar will grow, otherwise the bar volume will decay (transferring sediment to the berm). The change in bar volume (ΔV_B) during Δt is then given by:

$$\Delta V_{B,i}=\left(V_{BE,i}-V_{B,i}\right)(1-e^{-\lambda_i \Delta t}) \quad (5)$$

where subscript i denotes a certain time step. The new volume at time step i+1 is obtained from $V_{B,i+1}=V_{B,i}+\Delta V_{B,i}$. With the knowledge of the initial conditions (V_{B0}) and the input wave conditions, Eq. 5 can be used to calculate the evolution of the bar volume, both during growth and decay.

2.2. Theory for two bars

2.2.1. Two-bar evolution equation

Reports with focus on the response of multiple bar systems have been disseminated, *e.g.*, Lippmann *et al.* (1993); Ruessink and Kroon (1994); Wijinberg and Kroon (2002); Grunnet and Hoekstra (2004); Pruszak *et al.* (2008); Kroon *et al.* (2008); Różyński and Lin (2015); Aleman *et al.* (2017). Several theories have been advanced to explain the formation of longshore bars. Almar *et al.* (2010), for instance, concluded that the outer bar was most influenced by the offshore waves while the inner bar dynamics were most influenced by the tide range. However, when the outer bar undergoes a net offshore migration and degenerates, some authors report that the shoreline and inner bar are more exposed to wave energy and vulnerable to subsequent storm erosion (Price and Ruessink, 2011; Splinter *et al.*, 2016). Ruessink and Terwindt (2000) presented a conceptual model that describes the cyclic behavior of offshore migrating bars going through generation, seaward migration and decay stage. However, the inter-annual bar dynamics may vary considerably across sites with very similar environmental characteristics (Walstra *et al.*, 2016). According to Ruessink and Kroon (1994), bar parameters (such as volume, height, and mean water depth over the bar crest) can be well-linked to the bar stage. Larson and Kraus (1992) have also discussed correlations between bar and wave properties.

Important insights into the governing processes of interaction between the seabed and the wave forcing have been achieved by several authors regarding the behavior of longshore bars (Van Enckevort and Ruessink, 2003; Aleman *et al.*, 2015; Walstra *et al.*, 2016; Eichentopf *et al.*, 2018; van der Zanden *et al.*, 2017a,b; 2019). Walstra *et al.* (2012) has investigated a wave-averaged cross-shore process model to identify dominant mechanisms that govern bar amplitude growth and decay. However, due to the long duration of the tide cycle compared with the period investigated when testing model validity, the ability of wave-averaged process-based models has not been fully investigated (Kuriyama, 2012). To date, data studies are partially successful in explaining differences in the bar cycle return period, establishing at best weak correlations to local environmental settings (Walstra *et al.* 2016).

By analyzing the predictability of cross-shore sandbar behavior, with focus on cross-shore sandbar migration, Pape (2010) concluded that sandbars move toward a stable equilibrium location during breaking conditions. In this study, the type of bars that are empirically investigated are those formed by wave breaking on beaches exposed to moderate or high wave energy conditions with a moderate tidal variation. The condition for incipient breaking is a function of the local beach slope (accounted in a direct way by means of the equilibrium beach profile) and the wave steepness. The semi-empirical model developed for one-bar systems have been successfully applied to several sites, also in combination with a dune erosion model (Larson *et al.*, 2013; 2016), suggesting that this equilibrium approach may be also suitable to examine equilibrium behavior of other sand-bar systems. Pape (2010) found that short and small-scale nonlinear processes underlying sandbar migration drive a sandbar toward a wave-height-dependent equilibrium state that can, in principle, be predicted from the instantaneous wave height. Aiming to improve the one-bar model performance, a system consisting of two bars was studied, namely an inner and an outer bar. Here, a simple wave criterion is proposed for predicting the onshore and offshore movement of the inner and outer bar with reference to their equilibrium condition. As discussed by Wijnber and Kroon (2002), the response of the nearshore morphodynamic system is dominated by variation in the forcing of the system, and the response if more or less instantaneous. Following this theory, the proposed model assumes that when waves are small, only an inner bar forms. However, during high-energy wave conditions (*e.g.,* storms), large waves will break offshore and form an outer bar as well. These large waves will reform in the trough and eventually shoal and break again closer to the shore, resulting in a second but smaller inner bar in the same manner in which the most seaward main breakpoint bar was formed (Larson and Kraus, 1992). Dissipation of energy decreases in the reformed waves, implying a corresponding decrease in the sediment transport rate. The described mechanism is valid for both plunging and spilling breakers, although the time scale of bar development will be longer under spilling breakers (Sunamura and Maruyama, 1987). For a multi-bar model, a method or criterion is needed to define how many bars will form for certain wave conditions and sediment characteristics. At the present model development, since the focus is on a two-bar system, a simple approach is desirable and a criteria based on the wave characteristics is employed. If the incoming wave height is greater than a certain wave height (hereafter referred as the critical wave height, H_c) then two bars will develop, otherwise, when $H_0<H_c$, the system strives towards only one bar.

The bar volume, as in the one-bar system, is taken as indicator of the transport direction, where a growth in the outer bar volume is associated with a net seaward movement of sand and a decay in the outer bar volume is caused by onshore sediment movement (inducing degeneration of the outer bar). The build-up of the outer bar is taken as an intermittent process confined to the occurrence of high-energy periods, as also verified by Eichentopf *et al.* (2018) when studying the evolution of breaker bars under high energy (erosive) wave conditions. The model treats each bar as a discrete entity, allowing also feedback from adjacent features, although the migration of individual bars is not captured by the model.

It was earlier demonstrated by Larson *et al.* (2013, 2016) that the empirical equation for the equilibrium bar volume could be employed to calculate the total sediment volume stored in the inner and outer bar at Duck. Thus, this equation will be used for a multi-bar system to obtain the sum of the inner and outer bar volumes at equilibrium state. The normalized equilibrium bar volume is then given by,

$$\frac{V_{BE}^{TOT}}{L_0^2}=\frac{V_{BE}^{I}}{L_0^2}+\frac{V_{BE}^{O}}{L_0^2} \qquad (6)$$

where the superscript TOT, I and O denote total, inner, and outer equilibrium bar volume, respectively. The question arises on how to partition V_{BE}^{TOT} between V_{BE}^{I} and V_{BE}^{O}. Defining the ratio $\delta = V_{BE}^{O}/V_{BE}^{I}$, then:

$$V_{BE}^{I}=\frac{1}{1+\delta}V_{BE}^{TOT} \quad (7)$$

$$V_{BE}^{O}=\frac{\delta}{1+\delta}V_{BE}^{TOT} \quad (8)$$

These equations yield how much of the total bar volume belongs to the inner and outer bar, respectively. If δ can be predicted, by using Eqs. 7 and 8, V_{BE}^{I} and V_{BE}^{O} can be determined. At a first order approach, δ should depend on the relationship between H_0 and H_c; that is, a larger wave height with respect to the critical wave height (H_c) will produce a relatively larger offshore equilibrium bar volume. Based on this observation, the following empirical relationship is proposed:

If $H_0<H_c$, then $$\delta=0 \quad (9)$$

Otherwise, for $H_0>H_c$ $$\delta=\delta_0\left(\frac{H_0}{H_c}-1\right) \quad (10)$$

where δ_0 is an empirical coefficient to be calibrated against data (=1 as a first estimate). The subaqueous processes that build the two-bar system are represented in Figure 2. If $H_0<H_c$, then the outer bar will not form or will tend to disappear ($V_{BE}^{O}=0$), whereas $H_0>>H_c$ means that the outer bar will grow relatively larger in relation to the inner bar ($V_{BE}^{O}>>V_{BE}^{I}$).

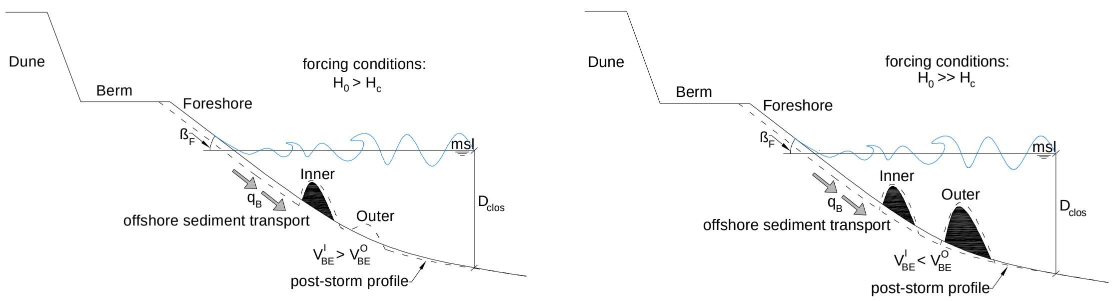

a) For 0<δ<1, the outer bar starts to form and grow.

b) For δ>1, the outer bar grows relatively larger than the inner bar.

Figure 2. Evolution model for a two-bar system.

2.2.2. Numerical solution

For each wave condition (at a specific time step), Eqs.7 and 8 together with Eqs.9 and 10 are solved numerically (Larson *et al.*, 2013). The change in the inner and outer bar volume is computed in the same manner as for the one-bar system using the analytical solution described in Eq.5,

$$\Delta V^{I}_{B,i}=\left(V^{I}_{BE,i}-V^{I}_{B,i}\right)(1-e^{-\lambda^{I}_{i}\Delta t}) \quad (11)$$

$$\Delta V^{O}_{B,i}=\left(V^{O}_{BE,i}-V^{O}_{B,i}\right)(1-e^{-\lambda^{O}_{i}\Delta t}) \quad (12)$$

where subscript i denotes a certain time step. The new volume at time step i+1 is obtained from $V^{I}_{B,i+1}=V^{I}_{B,i}+\Delta V^{I}_{B,i}$ (for the inner bar) and $V^{O}_{B,i+1}=V^{O}_{B,i}+\Delta V^{O}_{B,i}$ (for the outer bar). The λ coefficient, in Eqs.11 and Eq.12, will depend on whether the inner or outer bar grows or decays. However, as the inner and outer bars are located at different water depths, different behavior should be expected. According to Larson and Kraus (1992), once the outer bar is formed, it will only be exposed to wave breaking and large sand transport during severe storms, with the transport induced by non-breaking waves producing slower changes in the bar shape. On the other hand, the inner bar experiences wave breaking during most of the year, resulting in relatively faster response compared to the outer bar ($\lambda^{O}_{0} < \lambda^{I}_{0}$). Also, when onshore sediment transport and bar volume reduction occurs, a different multiplier ($\lambda^{on}_{0}=C_c\lambda_0$) to reduce the coefficient λ_0 should be adopted for the inner and the outer bar: $C^{I}_{c} > C^{O}_{c}$ (the values of these coefficients should be determined through calibration against data).

As an exchange of material continually takes place within the surf zone, depending on changes in the nearshore wave conditions, an exchange between the inner and the outer bar volumes can be considered in the calculations. Exchange of material between bars have been previously discussed by Wijnberg and Kroon (2002). According to these authors multi-bar systems may exhibit morphological feedback mechanisms affecting the response of the nearshore bars. This feedback consisting of local flow-topography interaction over individual bars but also interaction between bars. In this model, if no exchange of material is admitted between the inner and outer bar, the total bar volume going into or from the subaqueous portion of the profile is defined by:

$$q_B(t)=\Delta V^{TOT}_{B}/\,\Delta T,\ \text{where}\ \Delta V^{TOT}_{B} = \Delta V^{I}_{B} + \Delta V^{O}_{B} \quad (13)$$

The offshore or onshore sediment transport volume (from the berm to the bars or from the bars to the berm, respectively) is given by the sum of the total variation for both bars (inner and outer).

For cases where exchange of material between the bars is admitted, the outer bar volume variation is computed first (ΔV_B^O). Sediments are first transported to the inner bar when there is a net onshore sediment transport. If waves are forcing offshore sediment transport (ΔV_B^O>0), before compute the inner bar change (ΔV_B^I) it is determined whether the inner bar volume has enough sediment to provide to the outer bar, *i.e.*, if $V_{B,i-1}^I > \Delta V_{B,i}^O$. In case that this condition is not met, the inner bar volume will disappear totally ($V_{B,i}^I$=0) and the remaining sediment needed to fill the outer bar will be transported from the berm. For cases considering exchange of material between bars, total subaqueous volume is given by the inner bar volume change, $\Delta V_B^I/\Delta T$.

2.2.3. Equation for artificial bars (nearshore nourishments)

A simple approach is proposed to obtain a preliminary prediction of the migration rate of constructed sand mounds by numerically solving a schematic bar equation. The development of a criterion for predicting the evolution of nearshore mounds is based on the response of hypothetical outer bars subjected to transport by non-breaking and breaking conditions, that is, mounds placed within the surf zone, where the cross-shore morphological development can be dominated either by non-breaking or breaking waves. As a first approach, the study is focused on coastal systems with one natural bar (at most).

Considering the theory developed for systems characterized by the presence of two bars, different volumes can be modeled for the inner and outer bar. However, it was also shown that Eq. 6 can be employed when just one bar forms, where $V_{BE}^{TOT}=V_{BE}^I$ and V_{BE}^O=0. Due to the bar-berm coupling system, a continuous widening of the beach (or shoreline advance) is expected to occur. Based on that, Eq. 12 can be rewritten:

$$\Delta V_{B,i}^O=-V_{B,i}^O(1-e^{-\lambda_i^O \Delta t}) \quad (15)$$

According to Eq.15, the outer bar volume will tend to an equilibrium position characterized by the condition $V^{O}_{BE}=0$, leading to an uninterrupted onshore-directed sand movement.

Another important factor to take into account when reproducing the evolution of a feeder mound is the depth of placement because the morphological responses occurring along the sloping sea bottom are expected to be different as a result of changing sediment transport rates (Ruessink and Terwindt, 2000). If sand is placed at the top or seaward of the breaker bar or even in a more offshore position, a different impact or at least a different time adjustment towards equilibrium should be expected (Bodge, 1994). Ojeda *et al.* (2008), who studied the response of a two-barred system to a shoreface nourishment, based on a daily data set collected during about 6 years, refers that shoreface nourishment may enhance the possibility of bar switching by creating alongshore variability in the position and depth of the outer bar and in its cross-shore migration rate and direction. Ojeda *et al.* (2008) also concluded that the nourished sand may become part of the "natural" bar system, with minor offshore/longshore losses relative to the observed onshore effects. A rational simple criterion or method is desirable to determine the overall response of the artificial mound for the incoming waves. Through the study of the response of natural longshore bars, in particular the response of outer bars, Larson and Kraus (1992) have investigated different combinations of dimensionless parameters, such as, wave steepness, dimensionless fall speed and wave height over grain size diameter to develop a criterion that could distinguish accretionary and erosional events. Here, bar degeneration by depth-limited breaking waves is investigated through a simple approach based on wave height:

If $H_0<H_1$, then (calm wave conditions; non-breaking waves)

$$\Delta V^{O}_{B}=-V^{O}_{B,i}(1-e^{-\lambda^{O}_{1}\Delta t}) \ , \ \lambda^{O}_{1}=C^{O}_{C}\lambda_0 \qquad (16)$$

Else $H_0>H_1$ (breaking conditions)

$$\Delta V^{O}_{B}=0 \qquad (17)$$

where H_1 represents the wave height limit for the groups of waves that will break at depths where the outer bar is located. With the assumption that breaking waves are the main cause of bar formation and movement (or a limiting factor on the depth to the bar crest, h_c), the minimum depth over the bar should be of the same magnitude as the breaking wave height, H_b. Numerous formulas have been proposed to relate the breaking wave height to the water depth. Larson and Kraus (1989) found a relationship between the depth-to-bar crest (h_c) and the breaking wave height (H_b) based on analysis of profile change in LWT experiments:

$$h_c=0.66H_b \quad (18)$$

An example of how the profile may change the evolution of a nearshore sand mound for certain wave conditions is hypothesized. If the waves are small ($H_0<H_1$), it is assumed that non-breaking waves will act across the bar and the incident waves will break closer to the shore, promoting onshore sediment transport of the dumped material. During energetic conditions described by $H_0>H_1$, wave breaking prevails and the sediment transport will be considered to be offshore-directed, producing no variation in the offshore mound volume, $\Delta V_B^O=0$. Thus, during smaller waves the nearshore is intended to be "active" and designed to release sediments towards onshore, promoting accretion on the beach, whereas for wave heights larger than the breaking wave height, the nearshore mound is regarded to be stationary.

3. MODEL APPLICATION – CASE STUDIES

In this section, three field data sets collected at 3 different sites in the US coast are employed for model calibration and validation.

3.1. Duck, North Carolina, USA

3.1.1. Background and data employed

In order to illustrate the properties of the developed model, an example is provided to reproduce the evolution of two longshore bars (inner and outer) that usually appear in the nearshore at Duck, North Carolina, USA. Time series of waves and beach profiles measurements, collected 2-3 times per month by the Field Research Facility (FRF) of the U.S. Army Corps of Engineers, were used to model the volume of individual bars from 26-Jan-1981 to 28-Dec-1989.

The wave data employed were recorded with a waverider buoy located in 18 m water depth directly off the FRF research pier (Larson *et al.*, 2013). Beach profile data have been previously analyzed by Larson and Kraus (1992) to obtain detailed morphological properties of two bar features (inner and outer) with respect to a least-square fitted equilibrium profile to the computed average surveying profiles (including volumes and bar crest location). In Larson and Kraus (1992), bar volume was determined as the volume of sand above an equilibrium profile (m^3/m) and the depth to the bar crest was defined as the smallest depth across the bar. For more details about the method to compute the bar parameters from field data, consult Larson and Kraus (1992). The derived bar data were considered here for model calibration and validation.

Overall, two measurements periods were identified by Larson and Kraus (1992) during which the inner bar consistently moved offshore to become the outer bar. These periods were observed just after the surveys of 28-Sep-1981 and 09-Sep-1988, where the offshore-moving bar became the outer bar. Although a distinction between the inner and the outer bar is appropriate for modelling purposes, this division is not straightforward. In the two-bar model the buildup of the outer bar is taken as an intermittent process confined to the occurrence of high-energy periods ($H_0>H_c$). The question remains under which conditions the inner bar, during its migration stage, should be recognized as the outer bar. For that purpose, the depth to the bar crest was regarded as the decisive parameter. Based on the Larson and Kraus (1992) analysis of the FRF data, Figure 3 displays the volume and Figure 4 the bar crest depth for the inner and outer bars.

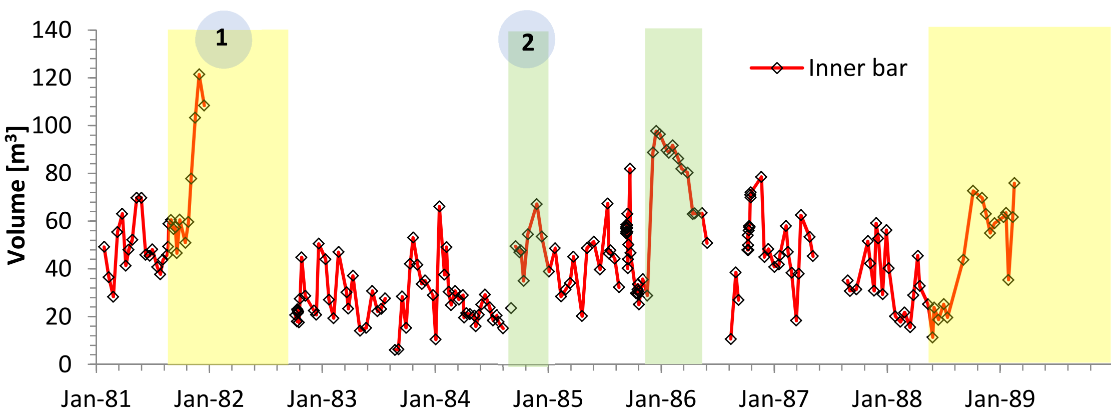

a) Inner bar

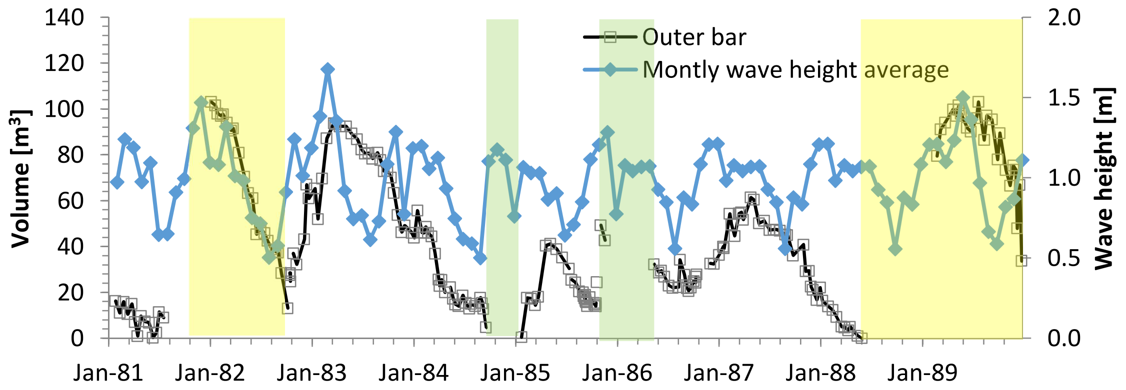

b) Outer bar

Figure 3. Volumes for inner and outer bar and monthly average of the measured wave height. Yellow shaded areas correspond to periods when the inner bar has migrated seaward to become the outer bar. Green shaded areas represent the periods when the outer bar has become flat but reappearing after that at the same location. Numbers 1 and 2 highlight the periods of profile surveying that are further down displayed in Figure 5a and Figure 5b, respectively.

Through analysis of the temporal variation in the observed outer bar volumes (see Figure 3), four cycles encompassing bar growth and decay can be identified during the measured period (1981-1989): 26-Jan-1981 to 17-Jul-1981, 07-Oct-1982 to 20-Sep-1984, 25-Jan-1985 to 21-Nov-1985 and 16-May-1986 to 02-Jun-1988. A detail analysis over these records can be consulted in Larson and Kraus (1992). These time periods were based on the first and last survey revealing an identifiable outer bar feature for time series of consecutive surveys with an outer bar present.

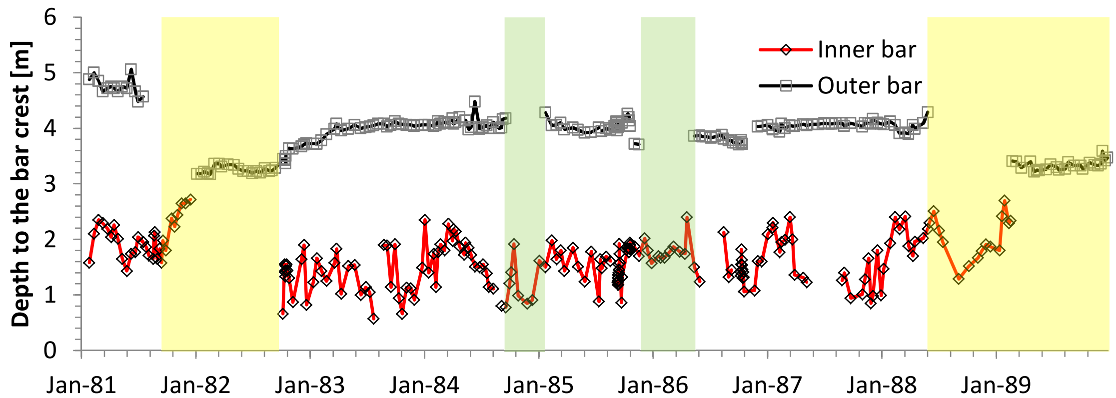

Figure 4. Depth of the bar crest for inner and outer bar. Yellow shaded areas correspond to periods when the inner bar has migrated seaward to become the outer bar. Green shaded areas represent the periods where the outer bar has become flat but reappearing after that at the same location.

As previously mentioned, after the outer bar disappeared, the offshore movement of the inner bar to become the outer bar was observed during two periods: 28-Sep-1981 to 07-Oct-1982 (see Figure 5a) and 09-Sep-1988 to 28-Dec-1989. Duck profile measurements have captured the termination of a bar cycle and the onset of the offshore migration of the inner bar from 28-Sep-1981 to 07-Oct-1982 and 09-Sep-1988 to 28-Dec-1989, providing an opportunity to evaluate the trigger point for a new cycle and its relationship to the outer bar response. Figure 5a displays times series of surveyed profiles collected between 28-Sep-1981 and 07-Oct-1982, where the onset of a new bar cycle can be distinguished.

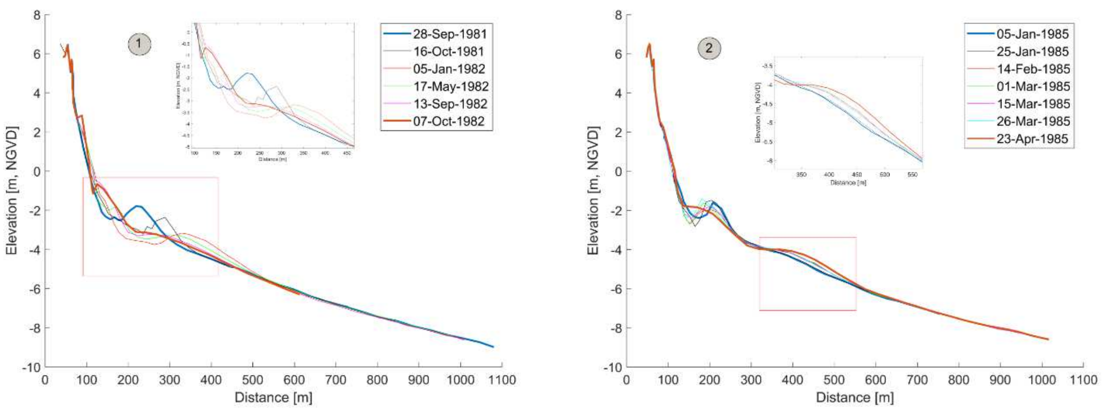

a) offshore progression of the inner bar to become the outer bar (28-Sep-1981 to 07-Oct-1982).

b) outer bar formation offshore (5-Jan to 23-Apr, 1985).

Figure 5. Surveyed profiles for Line 62.

The decay and growth of the outer bar was also observed during 20-Sep-1984 to 25-Jan-1985 and 21-Nov-1985 to 16-May-1986. However, during these periods no evidence was detected in the surveys regarding a cross-shore progression of the inner bar towards the outer zone. Instead, the observations indicated that the outer bar has regenerated itself and reformed in deeper water (see Figure 5b). This could be associated with more active sand transport promoted by a more frequent recurrence of breaking conditions, thereby affecting the transport and forcing of the outer bar, which starts growing (see large concurrent wave heights, Figure 3). Walstra *et al.* (2012) pointed out the longshore breaking wave induced currents as one of the mechanisms promoting bar decay and growth.

Figure 4 shows that the fluctuations of the outer bar crest location are significantly smaller and much more regular than the inner bar. It was decided that once a new bar has formed close to shore, and until it reaches the outer zone, the bar is taken as inner bar. In accordance with this criterion, bar measurements collected between 5-Jan-1982 to 13-Sep-1982 and 27-Feb-1989 to 28-Dec-1989 (periods during which the progressive bar experiences a stage described by small variations in position; see Figure 4), were assigned as outer bar observations. However, it has to be kept in mind that these assumptions were just defined for modelling purposes for comparing observations with the model results.

3.1.2. Model set up and calibration

The model was applied for the time period between 26-Jan-1981 and 28-Dec-1989, using wave measurements with a six-hour time step (Δt=6hr). The time series of the bar measurements were divided into two main periods, where the first one (extending from 1981-1985) was selected for calibration of the site-specific parameters (d_{50}, m, C_B, λ_0, δ_0, H_c) and the second one (from 1985-1989) was used for model validation. The values of the calibration parameters are presented in Table 1. Test calculations demonstrated that employing a smaller coefficient to quantify the bar response rate of the outer bar relative to the inner bar yielded improved agreement between calculated and measured bar volumes. As the inner bar varied more than the outer bar (see Figure 3), non-breaking conditions are also expected to produce slower changes in the outer bar shape. Thus, a different multiplier (C_c) to reduce the coefficient λ_0 during onshore sediment transport was introduced in the simulations for both bars.

The coefficient values expressing the inner and outer bar responses were assigned to minimize the least-square error (ε) defined as,

$$\varepsilon=\left(\frac{\sum_{i=1}^{N}\left(V_B^{obs}-V_B^{cal}\right)^2}{\sum_{i=1}^{N}\left(V_B^{obs}\right)^2}\right)^{1/2} \qquad (17)$$

where V_B^{obs} and V_B^{cal} represent the observed and calculated bar volumes, respectively. The initial bar volumes (t=0) were assigned to the initial observed values (calculated from the survey data). To test the model, two schematic cases were set up by switching on/off the exchange of material between the two bars.

Table 1. Site-specific calibration parameters, values of variables (Duck, N.C).

d_{50}	δ_0	H_c	T	m	C_B	λ_0^O	λ_0^I	C_c^O	C_c^I	V_B^o, t=0	V_B^I, t=0
mm	-	m	ºC	-	-	h^{-1}	h^{-1}	-	-	m^3/m	m^3/m
0.3	3	2	15	-0.5	0.08	0.0023	0.0036	0.15	0.75	49.2	16.2

Herein, to evaluate the skill of the model, two definitions were used to discuss the dispersion of the model results: least-square error (LSE, ε, Eq. 17) and normalized mean square error (NMSE, Eq. 18). Normalized square error is defined as (Poli and Cirillo, 1993):

$$\mathrm{NMSE}=\frac{\overline{\left(V_B^{obs}-V_B^{cal}\right)^2}}{\overline{V_B^{obs}}\,\overline{V_B^{cal}}} \tag{18}$$

where the overbar parameters ($\overline{V_B^{obs}}$ and $\overline{V_B^{cal}}$) represent the time mean bar volumes over the observed and calculated values. According to Splinter *et al.*, (2018), general skill assessment can be made by: NMSE<0.3 (*excellent*); 0.3<NMSE<0.6 (*good*); 0.6<NMSE<0.8 (*reasonable*); 0.8<NMSE<1.0 (*poor*). The least-square was taken as a complementary index to measure the dispersion of the model performance.

3.1.3. Results

Figure 6 illustrates the inner and outer bar volume variation with time and the agreement obtained with the observations during the calibration and validation periods, when no sediment exchange between the inner and outer bar was considered. The optimal parameter values found for 1981-1985, including the multiplier C_c for both bars, were used in the validation during 1985-1989.

Overall, promising results were achieved for the calculated outer bar volumes, yielding a least square error of ε=0.39, though the scatter obtained during the validation period was significantly larger compared with the calibration period. The NMSE obtained for the outer bar was 0.24, considered as '*excellent*' (NMSE<0.3). For the representative total volume stored in both bars (ε=0.51, NMSE=0.24), trends in volumes were reasonably reproduced showing a good initial agreement between the two series, but developing discrepancies towards the end of the validation period, corresponding to the time when the outer bar decayed and the inner bar experienced offshore migration (with only one bar appearing). The same is verified for the outer bar volume, with the largest deviation occurring during the summer of 1989, when the inner bar moved seaward as a result of the storms hitting the beach during the winter 1988/1989. A possible reason for the deviation might be the fact that wave conditions change faster than the time it takes for a sandbar to reach the equilibrium as also discussed by Pape (2010). Also, mainly during Sep-1989 the wave periods were considered unusually long (with an average and maximum value of 10.6 s and 23.3 s, respectively) and judged to be outside the range for which the estimated parameter values would be applicable. It should be emphasized that the model confines the outer bar growth to high-energy events, for which the input critical wave height assumes a central role (H_0>H_c). This site-specific parameter describes a change in the forcing conditions characterized by a stronger net seaward movement that would act as a trigger for the onset of the outer bar formation.

Due to the considerable scatter in the observations of the inner bar volume, demonstrating a quite random behavior, part of the data were poorly reproduced, with a computed least square error ε=0.55 (NMRSE=0.33, '*good*'). This may be attributed to the fact that the inner bar is typically located within the region of breaking waves, where profile changes are more irregular and with a rapid response, challenging the predictive capability of the model. Limitations on the predictability of the inner bar behavior were also recognized by Splinter *et al.* (2018) when applying a simple equilibrium model to field data of observed sandbar position.

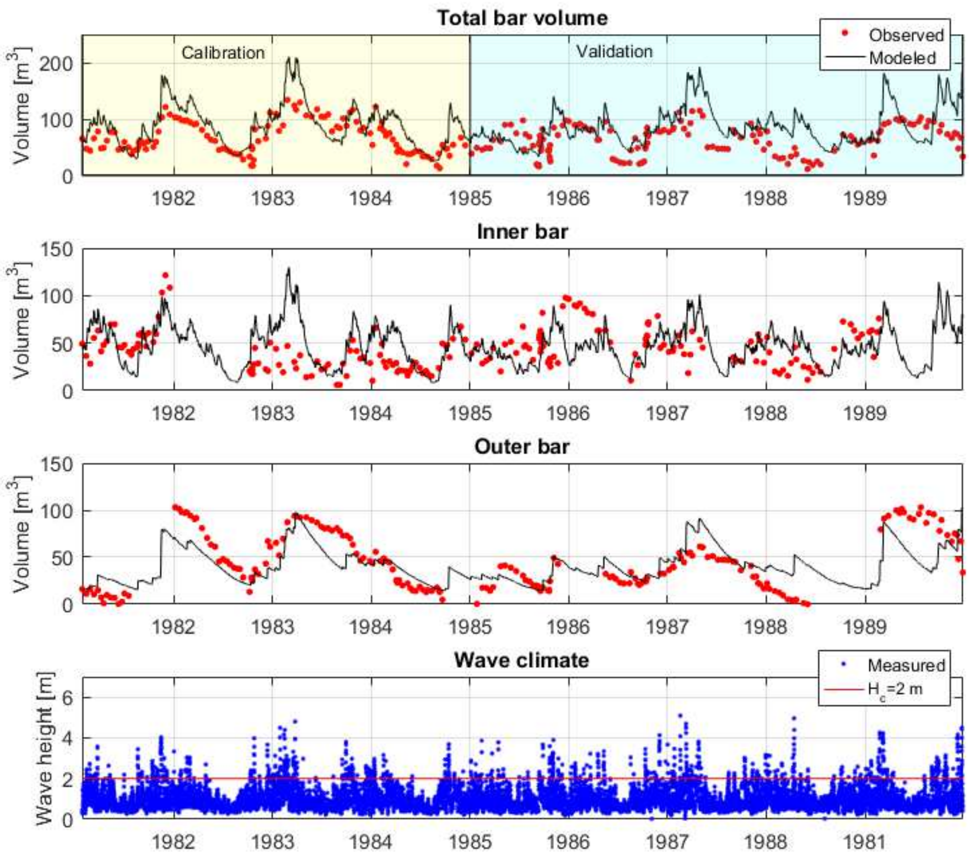

Figure 6. Total, inner, and outer bar volumes and wave climate (Duck, N.C.). Numerical simulations without considering sediments exchange between the inner and the outer bar.

Overall, comparing with the previous simulations, results including an exchange of material between the inner and the outer bar (Figure 7) produced the same main trends in bar volume change, but displaying changes in the inner and total bar volume, decreasing the least-square error to 0.51 (NMSE=0.29, '*excellent*') and 0.46 (NMSE=0.19), respectively. The assumption that sediment transported to the outer bar are coming from the inner bar, tends to smooth things out, decreasing the amount of sediment mobilized in the subaqueous portion by the waves and reducing the estimated amount of sediment being transported through the interface between the berm-bar region. Although a scatter is still noticeable for the inner bar volumes, the trends for total bar volume are reasonably well described, with the predicted sum of the calculated bar volumes approximating the measured values. Thus, the exchange of material between the bars yielded improved agreement.

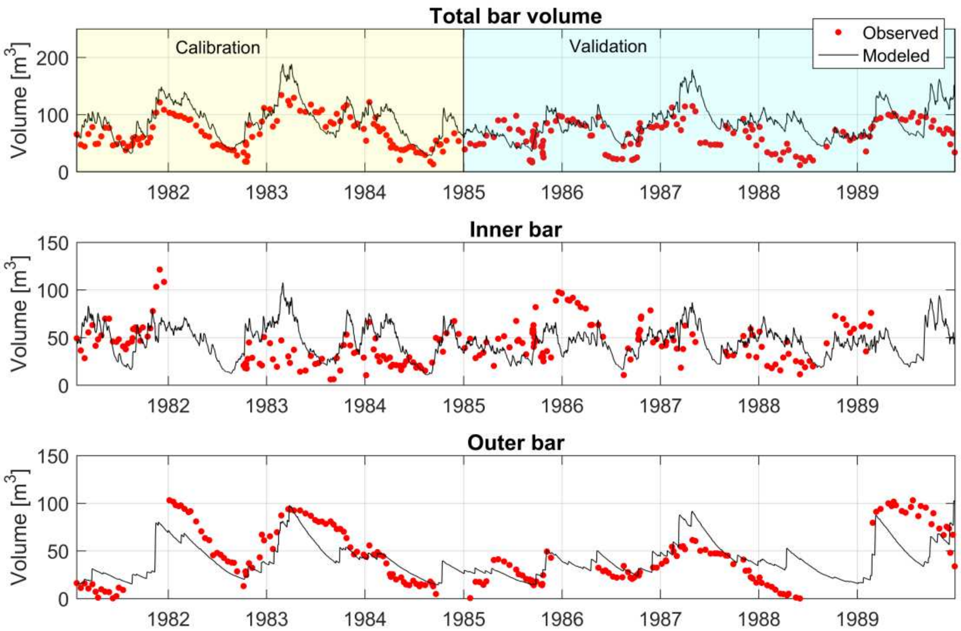

Figure 7. Total, inner, and outer bar volumes and wave climate (Duck, N.C.). Numerical simulations considering sediment exchange between the inner and the outer bar.

3.2. Silver Strand, Coronado, San Diego, California, USA

3.2.1. Background and data employed

The developed model for estimating the response of artificial nearshore bars intended to perform as feeder mounds is here employed for reproduction of a field experiment carried out at Silver Strand, San Diego, California. During Dec-88, dredged material removed from the outer portion of the channel entrance to San Diego Harbor was placed in the nearshore zone off Silver Strand State Beach (located approximately 7.5 km southeast of the dredging site) as a means of supplying the beach and preventing further erosion. The inlet-dredged sand was disposed at the top of an existing bar, between water depths ranging from -3 to -9 m MLLW (Mean Lower Low Water), creating a mound with dimensions approximately 360 m alongshore and 180 m across shore, and an average relief around 2 m. The estimated dredged amount was about 113 000 m^3, corresponding to an incremental cross-shore volume of 310 m^3 per m of shoreline. The mound was composed of medium sized sand (d_{50}=0.18 mm) according to Juhnke *et al.* (1989), whereas the median grain size of the native material was approximately 0.25 mm.

Repetitive cross-shore surveys covering the placement area were performed during almost one year after the project was completed (from 9-Dec-1988 to 15-Nov-1989). In total, 9 field campaigns were carried out for 7 profiles, in which four lines covered the initial location of the fill, and three were located southward. From the 9 campaigns, one was carried out just before (9-Dec-88) and one just after (29-Dec-88) the nearshore mound construction. These data have been earlier analyzed by several authors, so for more details consult Juhnke *et al.* (1989), Andrassy (1991), and Larson and Kraus (1992). According to Larson and Kraus (1992), all the survey lines located across the placement site displayed similar behavior. Figure 8a plots the surveys collected at a representative line during the first year, after the mound construction. Figure 8b displays the evolution of some nearshore bar properties (volume, maximum height, and depth to the bar crest) determined by Larson and Kraus (1992) by comparing the surveyed profiles with a derived equilibrium profile (obtained through least-square fitting of an equilibrium profile to the pre-construction survey). The bar volume (m^3/m) is given by the area of the surveyed profile above the equilibrium profile. The maximum bar height in Figure 8b is obtained as the largest vertical difference between the surveyed profile and the equilibrium profile.

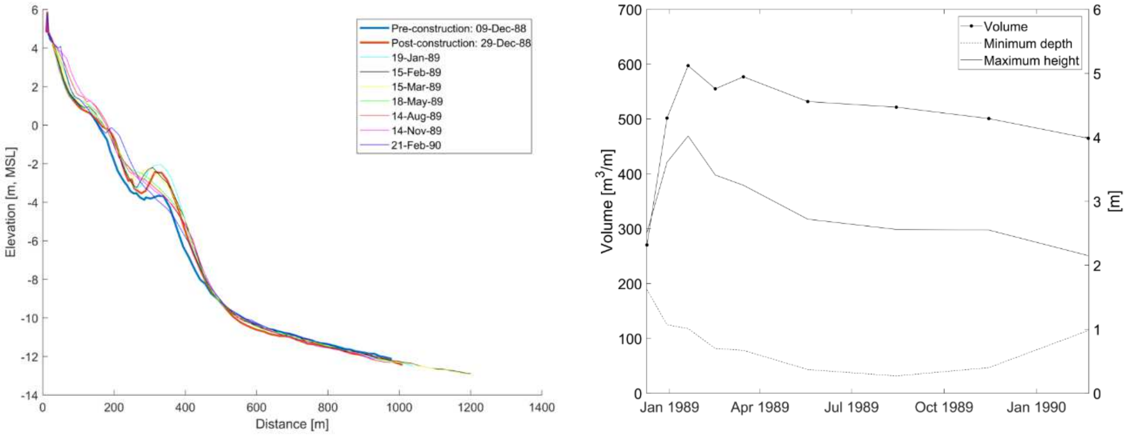

a) Surveyed profiles at Line 5 (during first year after mound construction).

b) Volume, maximum bar height and minimum bar depth (depths refer to MLLW, = MSL - 0.85 m).

Figure 8. Evolution of the nourishment operations.

As shown in Figure 8b, after the fill placement, the maximum bar height increased rapidly, but after about 5 months a constant value was approached, indicating that the bar primarily flattened out during this period – note the significant reduction in the mound relief from 4.02 (Jan-89) m to 2.72 m (May-89). Although less marked, the volume change follows the same trend as the observed bar height, reaching its maximum in Jan-89 with almost 600 m^3/m. The increase in material occurring between 29-Dec-1988 and 10-Jan-89 derived from clean-up dredging and disposal operations that were still conducted during this period as a result of a couple of hot spots remaining in the channel. It was estimated that approximately 7 650 m^3 of sand was dredged for that purpose. However, according to Andrassy (1991) the highest fraction of the deposition registered between the post-construction and the following survey was likely related to some accretion of sand moving alongshore as a result of the creation of a relative low energy area in the lee of the disposal site.

3.2.2. Model set up and calibration

The empirical approach described by Eq. 14 was adopted to simulate the evolution of the mound created off Silver Strand State Park, for the time period of 9-Dec-88 to 21-Feb-90. The input profile was schematized based on the pre-construction survey carried out in 9-Dec-88. In order to investigate model performance two schematic cases were set up: 1) simulating the fill operation due to instantaneous addition of material to the existing bar volume (inner), adjusting the bar response rate with respect to the general response of the mound; and 2) modelling a representative morphological volume of the inner portion of the profile, so that a transport of the fill material towards shallow depths, deriving from the flattening and onshore bar migration process, could be reproduced. Since wave measurements in connection with the surveys were only available for a limited time period (between 20-Jan-1989 and 18-May-1989), hindcasted wave data were employed in the simulations for the missing period. The model time step was set up based on WIS (Wave Information Studies) wave information, available every 3 hours. An extra cross-sectional fill volume of 71m^3/m was added to the simulations to represent disposal operations and longshore volume variations that occurred between 29-Dec-88 and 19-Jan-89. The values of the remaining site-specific input parameters were mainly determined by comparing results and trends of changes in bar volume in order to obtain the lowest value on ε for both the schematic cases. Based on the average value of the minimum depth to the bar crest, in the latter case, a wave breaking height H_1=0.8 m was specified to identify events when sand is transported onshore across the inshore portion of the profile.

Table 2. Site-specific calibration parameters, values of variables (Silver Strand, CA).

d_{50}	H_1	T	m	C_B	λ_0^I	C_c^I	V_B^I, t=0
mm	m	ºC	-	-	h^{-1}	-	m^3/m
0.2	0.8	15	-0.5	0.08	0.002	0.1 (Case1) -0.2 (Case2)	270

3.2.3. *Results*

The bar transport model was successfully employed for the one-year simulation period; the pattern of landward migration of the offshore mound could be reproduced for the studied profile. The results of the simulations are here presented and evaluated by comparing the computed bar volumes with the values on the offshore bar volume estimated from surveys (see Figure 9 and Figure 10).

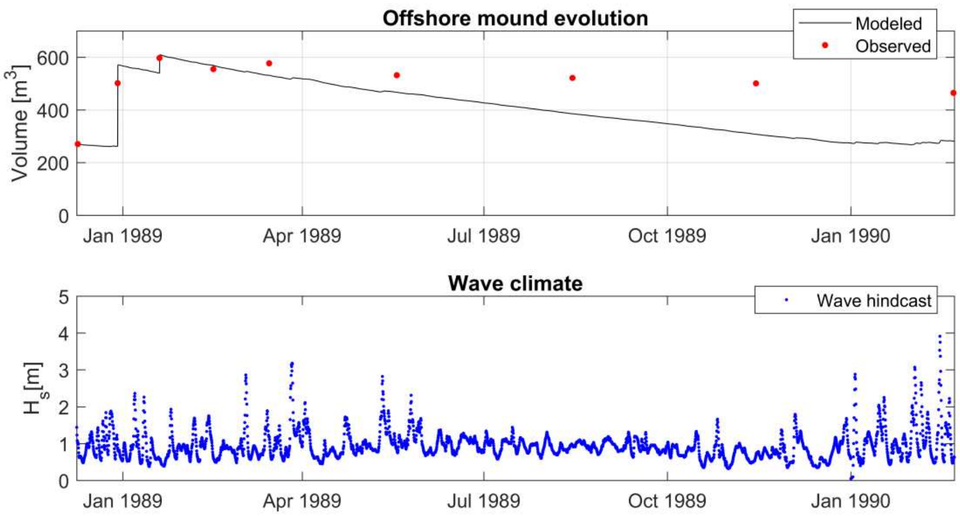

Figure 9. Nourishment evolution simulation by adding extra volume to the existing bar (Silver Strand, Coronado).

Figure 9 displays the simulation results obtained when directly adding material to the existing bar. As seen in the figure, discrepancies develop towards the end of the period of simulation, as the measured bar volume exceeded the predicted values. The computed error was ε=0.26 (NMSE=0.09), with an error for the last four data points computed in ε=0.30 and NMSE=0.12. The observed data points indicate that a large part of the fill material still remains at the site placement area, revealing that the model release the fill material from the bar towards the beach somewhat too quickly. The onshore transport of material captured by the surveys, exhibiting a gradual lowering of the maximum bar height, as well as an increase of material in the inshore portion of the profile might be a possible reason for obtaining these deviations (see Figure 5a for the behavior of the natural bar). Ojeda *et al.* (2008), when evaluating the response of a two-bar system, also detected that the shoreface nourishment performed in Noordwijk (The Netherlands) delayed the natural development of the two subtidal, with a marked decrease in the offshore migration rates for both the inner and outer bar. Figure 10 shows the model results when simulating a hypothetical inner feature to better account for the transfer of material across the surf zone. In this figure, the natural evolution of the nourished bar is represented by the dashed line (computed with respect to its equilibrium state). The green line represents the evolution of the hypothetical feature which depends on low-energy events ($H_0<H_1$) to transport the fill material to the beach. The continuous black line corresponds to the sum of the modeled values for the inner portion volume and the nourished bar volume. Although the surveys have indicated a mixed response between the existing bar and the fill volume (moving as an unique

identifiable unit), the calculations demonstrate that simulating the impact of flattening mound process by incorporating a hypothetical inner feature produced significant improvement, especially during the final part of the study period where measured and modeled values agree well, yielding a lower total error of ε=0.18 (NMSE=0.03, considered '*excellent*'). Also, the trends are satisfactorily described, making the reproduction of the measurements better than in Figure 9.

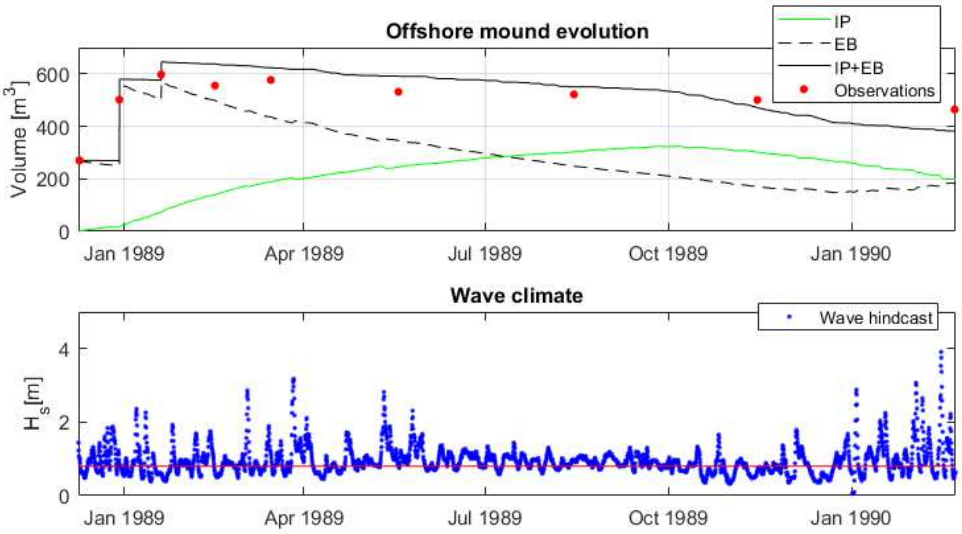

Figure 10. Nourishment simulation using a representative volume for the inner portion (Silver Strand, Coronado), where IP and EB are acronyms for Inshore Portion and Existing Bar (nourished with dredged material), respectively. Red line represents a threshold for the wave height that controls when sand is transported landward, from the inner portion of the profile to the berm (H_1).

3.3. Cocoa Beach, Canaveral, Florida, USA

3.3.1. Background and data employed

Here, the model applicability in predicting the evolution of a sand bar artificially implemented at Cocoa Beach (Florida, USA), a coastal area where natural breaker bars were not observed, is demonstrated. Dredged sand from 1992-1994 maintenance activities at the Port Canaveral Entrance channel was placed in a nearshore disposal area offshore of Cocoa Beach (8.4 to 11.3 kilometers southward of the source), in order to retain beach-compatible sand in the littoral system. The fill activities started in 1992 (from 6-June through 24-Jul), involving the deposition of 121 000 m^3 of sand. In 1993 and 1994, more disposal activities were undertaken, implying a total sand volume mobilized of around 263 000 m^3. A specific set of high-quality monitoring data related to the first intervention (1992) were selected for model application. This data set encompasses five bathymetric surveys collected for several lines alongshore, spaced about 40 to 75m apart, intercepting the placement site. These lines were surveyed before (pre-project, Jun-1992) and after the fill placement (post-project, Jul-1992) and then on three different occasions until one year after construction was completed (Dec-92, May-93, Jul-93). The data collection extended from 45m seaward of the disposal area to about 245m landward thereof, or from the -8.4m to -3.4m MLW (Mean Low Water) depth contours. According to Bodge (1994) the permitted nearshore disposal area of 1992 was defined 2 895m in the longshore direction and 200 to 245m wide in the cross-shore direction. Figure 11 depicts the surveyed profiles along two distinct lines: one located in the northern part of the designated placement area and the other in the southern part, where no fill material was placed during the first disposal.

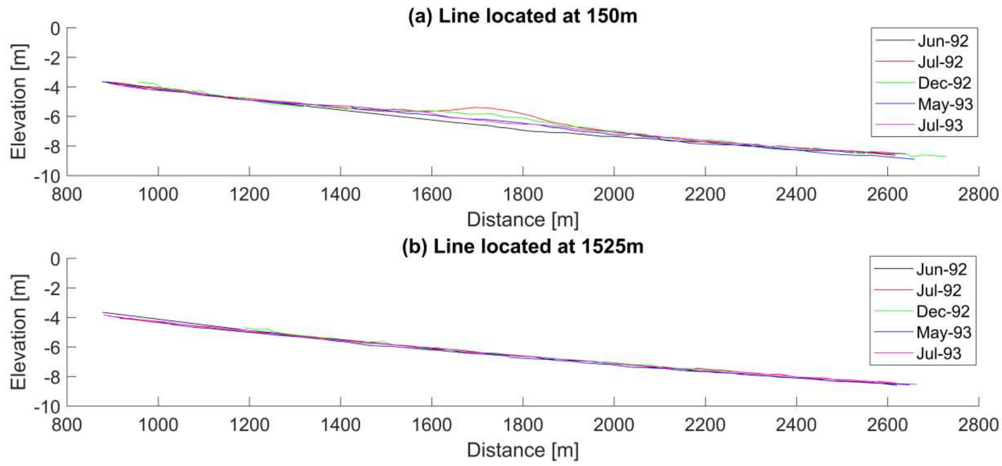

Figure 11. Selected survey profiles intercepting the permitted disposal area (0m to 2 895m in the local alongshore coordinate system): (a) northern part and (b) southern part.

Although the authorized disposal area extended alongshore from station 0 southward to station 2895 (0m to 2895m in the local alongshore coordinate system), inter-survey data analysis along this area showed that the nourishment activity focused in the north, from station 0 to about 815m southward. This is in agreement with Figure 11, where the seabed changes of the most northern-located profile (Figure 11a) demonstrates that the initial bar was constructed here, while no pronounced bar is observed in the southern disposal area (Figure 11b). Thus, since the nourished sand was not uniformly distributed alongshore in the permitted dumping area, six northern evenly-spaced profile lines were selected to evaluate the seabed changes associated with the nearshore bar. For each survey event, the average depth of these six profile lines (intercepting the disposal activity) was computed; the evolution in time was thereafter compared within the same cross-shore surveyed area (located between 320m and 790m – distance to an artificial baseline being approximately the NGVD – National

Geodetic Vertical Datum – shoreline). Since the first survey was carried out before the fill placement, the corresponding average profile was designated as the "background" (or "pre-project") profile. Figure 12 plots the average profiles computed for each survey event that occurred between 16-Jun-1992 and 1-Jul-1993.

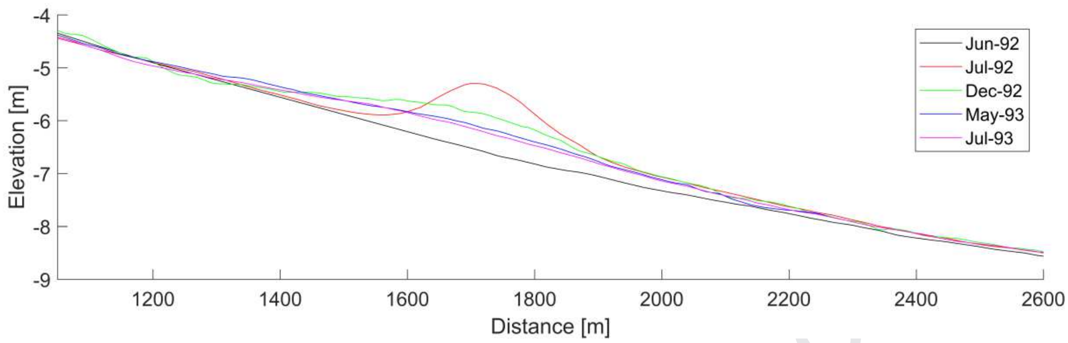

Figure 12. Average profile evolution at northern disposal area (0m to 800m). Distance along the profiles refers to an artificial baseline set at approximately the NGVD shoreline. Elevation in relation to NGVD.

In Figure 12, an artificial nearshore bar can be recognized just after the placement (Jul-92), as well as a subsequent pronounced landward migration of the mound during the following months (Dec-92; May-93; Jul-93) accompanied by a clear shift of the bar crest towards shallower waters. Overall, the onshore movement of the artificial bar resembles a cross-shore diffusion process, influenced by a shoreward-directed advection. Thus, the flattening and onshore movement of the mound contributed to the accretion of material along the inner portion of the profile.

3.3.2. Model set up and calibration

The model was run for a year, from 16-Jun-1992 to 01-Jul-1993. The numerical model was set up to reproduce the behavior of the nearshore mound disposal through the simulation of a schematic feature defined by $V_{BE}^{O} = 0$ (representing the outer portion of the profile). In line with the Silver Strand study case, to better reproduce the transport of the fill material through the surf zone (Figure 12), a representative morphological volume for the inshore area was included in the simulations. This morphological feature, included to describe the exchange of material between the subaqueous bar and shallower portions of the profile, was considered to behave in the same manner as the outer bar, implying a second threshold value for the wave breaking height, H_{b2}, intended to control the nearshore activity. Both equilibrium volumes are set to be zero and thus, this exchange of material is considered to be onshore-directed. Since no wave measurements were made in connection with the profile surveying, a wave hindcast with a 3-hour time step was used in the simulations. Model calibration was performed by adjusting site-specific input parameters and estimated values based on the pre-surveyed profiles and previous studies. According to Bodge (1994), as the native grain size (0.104 mm) differed significantly from the nourished sand (0.40 mm), an average value of 0.21 mm was adopted for d_{50}. The same parameters values on m, C_B and λ_0 used for Silver Strand were kept for Cocoa Beach. The optimal value on the multiplier (C_C) employed to reduce λ_0 was 0.2. To validate the model, comparisons were made with measured profiles.

Table 3. Site-specific calibration parameters, values of variables (Cocoa Beach, FL).

d_{50}	H_{b1}	H_{b2}	T	m	C_B	λ_0^I	C_c^I	V_B^0, t=0
mm	m	m	ºC	-	-	h^{-1}	-	m^3/m
0.21	4.2	2.0	26	-0.5	0.08	0.002	0.2	0

3.3.3. Results

The model results were quantitatively evaluated by comparing the computed bar volumes with the values estimated from the surveys. Figure 15 depicts the time variation in the calculated bar volume, as well as the agreement obtained between the measured and the predicted values during the first year after nourishment operations.

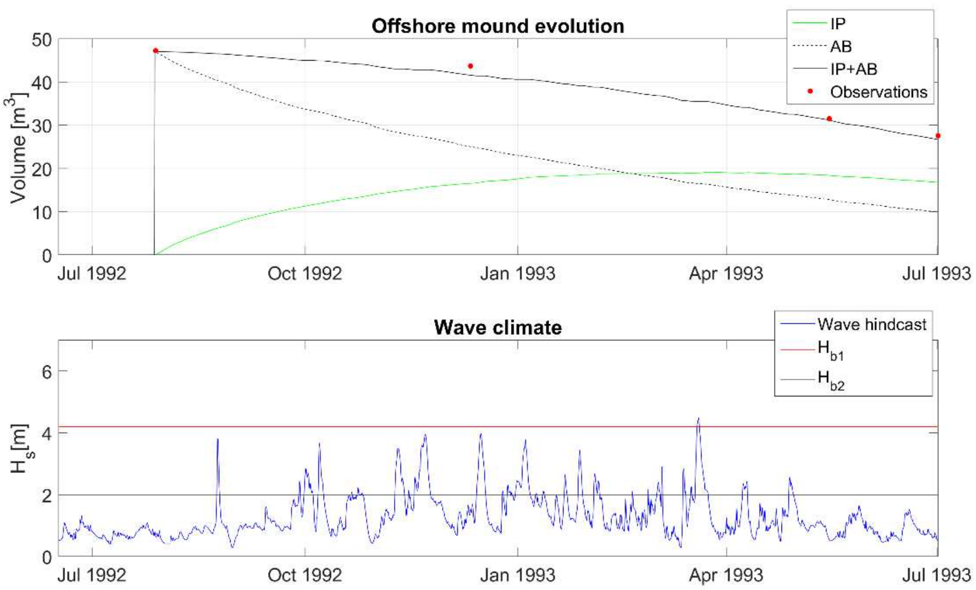

Figure 15. Results of the nourishment simulation using a hypothetic outer bar (Canaveral, Cocoa Beach) considering exchange of material with the inner portion of the profile. The green shaded area represents the period of measurements.

The model prediction is judged to be good by considering the transfer of fill material towards the shore through the most inshore portion of the profile. The obtained error was ε=0.03 (NMSE=0.001, '*excellent*' agreement). At the same time as the outer bar started to release sediment, the inner portion filled up as the wave forcing was favorable for such conditions (note that the wave climate was quite energetic during this period). A shift towards low-energy wave conditions (reflected by a general decrease of the values of H_s) appearing simultaneously with the maximum inner volume (Apr-93) suggests a change to a negative sediment budget at the inshore part of the profile, where the volume transported from the outer zone to the inner becomes lower than the volume transported from the inner portion to the beach (see Figure 15). This behavior is in agreement with Figure 12, where the major modifications of the mound shape took place during the first 5 months just after the fill placement (between the "post-survey" and Dec-92), while during the next period (Dec-92 to May-93) a higher volume loss occurred. Overall, the time adjustment of the profile towards an equilibrium state is being properly described by the model, as well as the volume time variation during the measurement period.

3.4. DISCUSSION

The model application at three different study sites (Duck, Silver Strand, Cocoa Beach) showed that the equilibrium bar model is skilled at predicting the time-varying volume of the outer bar, suggesting that this morphological feature is strongly influenced by offshore wave forcing in a predictable, equilibrium-forced manner (ε=0.39; NMSE=0.24). Model skill was lower when predicting the inner bar. It is yet to be explored if the inner bars in a multi-bar sites display predictable, equilibrium driven cross-shore behavior, similar to outer bars and shorelines. According to Splinter *et al.* (2018), the behavior of the inner bars is hypothesized to be more conditioned by changes in the tide range and act as sediment transport pathways between the shoreline/berm and the outer bar. Duck measurements have detected that some bars form in the nearshore and move all the way offshore (eventually deflating by non-breaking waves). During those periods, results demonstrated a decrease in model performance. This might be attributed to the fact that bars are mostly out-of-equilibrium with the wave conditions, since wave climate change faster than the time it takes for a sandbar to reach the equilibrium state as also discussed by Wijnberg and Kroon (2002) and Pape (2010). Pape (2010) referred that long-term offshore-directed trends in sandbar location develop when sandbars never reach the equilibrium locations associated to the highest waves. As result, the trends in this type of sandbar behavior are difficult to reproduce because the nonlinear nature of the underlying physical processes may cause exponential error accumulation over time (Pape, 2010). The developed model, rather than resolve the fine details of the profile response (or bar shape/location), relies on a simple equilibrium approach to compute volume changes distributed between the two bars, responding each one to the wave forcing at the input time scale. It was equally observed in Duck data that a lot of inner bars form in shallow water do not move offshore, but remain as inner bars all the time. In the developed model, the inner bar will not become the outer bar, but material previously dedicated to the inner bar will be available for the outer bar. Increase of bar volume is mostly linked to situations with severe surf zone conditions promoted by high-energy events, as also observed and discussed by Ruessink *et al.* (1994, 2007, 2009) and Grunnet and Hoekstra (2004) during the migration stage of the bars. According to Pape (2010), sandbars that do reach their equilibrium during a storm, do not show any trends longer than the duration between individual storms.

Overall, equilibrium volumes and rate-of-change coefficients were related to non-dimensional wave and sediment properties (*i.e.*, wave steepness and non-dimensional fall speed), but during the calibration certain non-dimensional multipliers (or coefficients) in the empirical transport relationships had to be obtained through comparison with data and subsequently validated. Although the criteria presented here should provide a first rough estimate of suitable values, parameters such as the critical wave height and wave breaking height (used to define the wave heights thresholds for bar formation and development), are expected to be site-specific and data are needed to apply the model with confidence at a particular site.

The low temporal resolution of the data employed for Silver Strand and Cocoa Beach case studies (approximately one year) was considered a limitation to this study. Modelling of multi-bar system is complicated when bars merge naturally or artificially (as a result of nourishment operations) and migrate both in time and cross-shore. Although bar morphology and its dynamic response have been extensively investigated in the last years by several authors (Van Enckevort and Ruessink, 2003; Ruessink *et al.*, 2009; Pape, 2010; Walstra *et al.*, 2012; Aleman *et al.*, 2015; Walstra *et al.*, 2016; Eichentopf *et al.*, 2018), bringing new findings from numerical and field observation studies about the dominant variables influencing the bar cycle duration (*e.g.*, grain size, bar characteristics, wave forcing and profile shape) and its cross-shore and longshore variability, models still need to be improved to fully address the physical processes responsible for bar development, establishing relationships between aggregated short-term processes and phenomenological medium-term bar behavior.

4. CONCLUSIONS

An extended version of the heuristic model, first introduced by Larson *et al.* (2013), was developed to reproduce the overall shift in material between the subaerial and subaqueous portions of the profile by taking into account the long-term evolution of multi-bar systems and the response of artificial bars resulted from nearshore nourishment operations. The model is based on simplifications of the governing processes, where bar volume evolution determines the transport direction. The model was successfully calibrated and validated in standalone mode at three field sites from the United States: 1) Duck, NC, where two natural longshore bars typically form and 2) Silver Strand, CA; and 3) Cocoa Beach, FL, where the evolution of offshore feeder mounds were surveyed.

One of the strengths of the model relies on the definition of an equilibrium state that is compared to the current state and some magnitude of forcing available to drive the changes in the profile. The methodology employed here allowed to quantitatively reproduce the main trends in the subaqueous beach profile response in a long-term perspective as a function of the bar volumes disequilibrium, the magnitude of the incident wave height and the dimensionless fall velocity to move the sand with a time-varying forcing term outside the disequilibrium term. In the presented model, each bar is treated as a discrete entity, allowing feedback from adjacent features, although the migration of individual bars is not captured by the model.

The model has shown some potential to predict the evolution of nearshore nourishments that migrate towards the shore and become part of the beach face by the action of waves and currents on beaches exposed to moderate or high wave energy conditions with a moderate tidal variation. This equilibrium modelling approach could be more widely applied to other beaches to explore shoreline equilibrium behavior, by merging it with a shoreline evolution model, or combining it with a compatible dune erosion module to simulate beach berm response and illustrate its applicability in predicting seasonal changes, as well as the supply effects at medium-term related to the fill project on the shoreline position. Future steps could also be directed to refine this bar model in order to include some parameterization of the bar shape, involving for instance a fixed shape (e.g. triangular) with specific height and length to characterize the bar as well as its migration toward a wave-height-dependent equilibrium location as concluded by Pape (2010) to be successful on predicting relevant features of long-term sand bar behavior, yearly and interannual trends.

Acknowledgements

This work has been supported by Fundação para a Ciência e Tecnologia through the PhD grant SFRH/BD/95894/2013.

REFERENCES

Aleman, N., Certain, R., Robin, N., Barusseau, J. (2017). Morphodynamics of slightly oblique nearshore bars and their relationship with the cycle of net offshore migration, Marine Geology, Volume 392, 41-52 pp.

Almar, R., Castelle, B., Ruessink, B., Sénéchal, N., Bonneton, P., Marieu, V. (2010). Two- and three-dimensional double-sandbar system behavior under intense wave forcing and a meso-macro tidal range. Cont. Shelf Res. 30 (7), 781–792.

Andrassy, C. J. (1991). Monitoring of a Nearshore Disposal Mound at Silver Strand State Park. Proceedings Coastal Sediments '91, American Society of Civil Engineers, pp 1970-1984.

Barnard, P.L.; Hanes, D.M.; Lescinski, J.; Elias, E. (2007) Monitoring and modeling nearshore dredge disposal for indirect beach nourishment, Ocean Beach, San Francisco. Proceedings 30th Coastal Engineering Conference, ASCE, 4192-4204.

Bodge, K. (1994). Performance of nearshore berm disposal at Port Canaveral, Florida. Proceedings, Dredging'94, American Society of Civil Engineers (ASCE) Specialty Conference, Orlando, Florida; November 13-16, 10 p.

Bouvier, C., Balouin, Y., Castelle, B. (2017). Nearshore bars and nearshore dynamics associated with the implementation of a submerged breakwater: topo-bathymetric analysis and video assessement at the Lido of Sète beach. Proceedings of the Coastal Dynamics 2017, Helsingør, Denmark, Paper no.22, 10 p.

Coelho, C. (2005). Riscos de Exposição de Frentes Urbanas para Diferentes Intervenções de Defesa Costeira. PhD Thesis, University of Aveiro, 405 p.

Davidson, M., Splinter, K., Turner, I. (2013). A simple equilibrium model for predicting shoreline change, Coast. Eng. 73, 191-202 pp.

Dean, R. (1987). "Coastal Sediment Processes: Toward Engineering Solutions," Proceedings of Coastal Sediments '87, American Society of Civil Engineers, pp 1-24.

DHI (2008). DHI-Profile Development, LITPROF User Guide.

DHI (2009a). LITPACK: An Integrated Modeling System for Littoral Processes and Coastline Kinetics (Short Introduction and Tutorial), published by MIKE, DHI.

DHI (2009b). LITLINE: Coastline Evolution (LITLINE User Guide), published by MIKE, DHI.

DHI (2017). Littoral Processes FM, All Modules, Scientific Documentation, 104 p.

Deltares (2011). UNIBEST-CL+ manual. Manual for version 7.1 of the shoreline model UNIBEST-CL+

Eichentopf, S., Cáceres, I., & Alsina, J. M. (2018). Breaker bar morphodynamics under erosive and accretive wave conditions in large-scale experiments. Coastal Engineering, 138, 36–48.

Gravens, M., Ebersole, B., Walton, T., Wise, R. (2003). Beach Fill Design. Coastal Engineering Manual, Part V: Coastal Project Planning and Design, Chapter 4, U.S. Army Corps of Engineers, Washington, DC, 113 p.

Grunnet, N., Hoekstra, P. (2004). Alongshore variability of the multiple barred coast of Terschelling, The Netherlands, Marine Geology 203, 23-41 pp.

Hanson, H. (1988). GENESIS-A generalized shoreline change numerical model. Journal of Coastal Research, 5 (1), 1–27 (Charlottesville, Virginia. ISSN 0749-0208).

Howd, P. A., and Birkemeier, W. A. (1987). Beach and Nearshore Survey Data: 1981-1984 CERC Field Research Facility, Technical Report CERC-87-9, Coastal Engineering Research Center, US Army Engineer Waterways Experiment Station, Vicksburg, MS.

Juhnke, L., Mitchell, T., and Piszker, M. J. (1989). Construction and Monitoring of Nearshore Disposal of Dredged Material at Silver Strand State Park, San Diego, California. Proceedings of the 22nd Dredging Seminar, Texas Engineering Experiment Station, CDS Report No. 317, pp 203-217.

Juhnke, L., Mitchell, T., and Piszker, M. J. (1990). Construction and Monitoring of Nearshore Placement of Dredged Material at Silver Strand State Park, San Diego, California. Dredging Research Technical Notes, DRP-1-01, pp. 1-11.

Kroon, A., Larson, M.,Möller, I., Yokoki, H., Różyński, G., Cox, J., Larroude, P. (2008). Statistical analysis of coastal morphological data sets over seasonal to decadal time scales. Coastal Engineering, Volume 55, Issue 7-8, 581-600 pp.

Kuriyama (2012). Process-based one-dimensional model for cyclic longshore bar evolution, Coastal Engineering 62, 28-61 pp.

Larson, M., Kraus, N.C., (1989). SBEACH: Numerical model for simulating storm-induced beach change, Report 1: Empirical foundation and model development. Technical Report CERC-89-9. U.S. Army Engineer Waterways Experiment Station, Coastal Engineering Research Center, Vicksburg, MS.

Larson, M., Kraus, N.C., (1992). Analysis of cross-shore movement of natural longshore bars and material placed to create longshore bars. Technical Report DRP-92-5. U.S. Army Engineer Waterways Experiment Station, Coastal Engineering Research Center, Vicksburg, MS.

Larson, M., Kraus, N. (1994). Temporal and spatial scales of beach profile change, Duck, North Carolina, Marine Geology 117, 75-94 pp.

Larson, M., Hanson, H., Kraus, N., Newe, J. (1999). Short- and Long-Term Responses of Beach Fills Determined by EOF Analysis. Journal of waterway, Port, Coastal, and Ocean Engineering, 285-293.

Larson M., Hanson H., Palalane J., (2013). Simulating cross-shore material exchange in long-term coastal evolution models. Proceedings of the Coastal Dynamics 2013, Arcachon, France, 1037-1048 pp.

Larson, M., Hanson, H. (2015). Model of the evolution of mounds placed in the nearshore. Journal of the Integrated Coastal Zone Management, 15 (1): pp 21-33.

Larson, M., Palalane, J., Fredriksson, C., Hanson, H., (2016). Simulating cross-shore material exchange at decadal scale. Theory and model component validation. Coastal Engineering, 116, 57-66.

Lipmann, T., Holman, R., Hathaway, K. (1993). Episodic, Nonstationary Behavior of a Double Bar System at Duck, North Carolina, U.S.A., 1986-1991, Journal of Coastal Research, SI 15, 49-75 pp.

Marinho, B., Coelho, C., Larson, M., Hanson, H. (2017a). Short- and long-term responses of nourishments: Barra-Vagueira coastal stretch, Portugal. Journal of Coastal Conservation, 15 p.

Marinho, B., Coelho, C., Larson, M., Hanson, H. (2017b). Simulating cross-shore evolution towards equilibrium of different beach nourishment schemes. Proceedings of the Coastal Dynamics 2017, Helsingør, Denmark, Paper no.121, 15 p.

Marinho, B., Coelho, C., Larson, M., Hanson, H. (2018a). Modelação Numérica da Aplicação de Dragados no Reforço do Perfil Transversal de Praia, Chapter III.3, pp. 131-151 pp. ISBN 978-972-789-535-9

Marinho, B., Coelho, C., Larson, M., Hanson, H. (2018b). Monitoring the Evolution of Nourished Beaches Along Barra-Vagueira Coastal Stretch, Portugal. Ocean & Coast. Manag., 157, 24-39 pp.

Palalane, J., Fredriksson, C., Marinho, B., Larson, M., Hanson, H., Coelho, C., (2016). Simulating cross-shore material exchange at decadal scale. Model application. Coastal Engineering, 116, 57-66.

Pape, L. (2010). Predictability of nearshore sandbar behavior. PhD thesis, Utrecht University, 160 p.

Pelnard-Considere, R. (1956). Essai de Theorie de 1' Evolution des Forms de Rivages en Plage de Sable et de Galets. 4th Journees de l'Hydralique, Les Energies de La Mer, Question III, Rapport 1, pp. 289–298.

Poli, A., Cirillo, M. (1993). On the use of the normalized mean square error in evaluating dispersion model performance, Atmospheric Environment, 27ª, 15, 2427-2434 pp.

Price, T.D., Ruessink, B.G., (2011). State dynamics of a double sandbar system. Cont. Shelf Res. 31 (6), 659–674. http://dx.doi.org/10.1016/j.csr.2010.12.018.

Pruszak, Z., Różyński, G., Szmytkiewicz, P. (2008). Megascale rhythmic shoreline forms on a beach with multiple bars, Oceanologia, Volume 50, Issue 2, 108-203 pp.

Roelvink, J.A., Reniers, A., van Dongeren, A.R., van Thiel de Vries, J.S.M., McCall, R., Lescinski, J., (2009). Modeling storm impacts on beaches, dunes and barrier islands. Coastal Engineering, 56, 1133–1152.

Różyński, G. and Lin, G. (2015). Data-Driven and Theoretical Beach Equilibrium Profiles: Implications and Consequences. Journal of Waterway, Port, Coastal, and Ocean Engineering, Volume 141(5), 17p.

Ruessink, B., Kroon, A. (1994). The behavior of a multiple bar system in the nearshore zone of Terschelling, The Netherlands: 1965-1993. Marine Geology, 121, pp 187-197.

Ruessink, B., Terwindt, J. (2000). The behavior of nearshore bars on the time scale of years: a conceptual model. Marine Geology, 163, pp 289-302.

Ruessink, B.G., Kuriyama, Y., Reniers, A.J.H.M., Roelvink, J.A., Walstra, D.J.R., (2007). Modeling cross-shore sandbar behavior on the timescale of weeks. Journal of Geophysical Research-Earth Surface 112 (F3), 1–15. doi:10.1029/2006JF000730.

Ruessink, B.G., Pape, L., Tumer, IL, (2009). Daily to inter-annual cross-shore sandbar migration: observations from a multiple sandbar system. Continental Shelf Research 29: 1663-1677 pp.

Ruggiero, P., Kaminsky, G., Gelfenbaum, G., Cohn, N. (2016). Morphodynamics of prograding beaches: A sysnthesis of seasonal- to century-scale observations of the Columbia River littoral cell, Marine Geology 376, 51-68 pp.

Splinter, K., Turner, I., Reinhardt, M., Ruessink, G. (2016). Rapid adjustment of shoreline behavior to changing seasonality of storms: observations and modelling at an open-coast beach. Earth Surf. Process. Landf. Splinter, K., Gonzalez, M., Oltman-

Smith, E., D'Alessandro, F., Tomasicchio, G., Cailani, J. (2017). Nearshore placement of a sand dredged mound. Coastal Engineering, 126, pp 1-10.

Sunamura, T. (1975). A study of Beach Rodge Formation in Laboratory, Geographical Review of Japan, 48-11, 761-767 pp.

Sunamara, T. and Maruyama, K. (1987). Wave-induced geomorphic response of eroding beaches – with special reference to seaward migrating bars. Proceedings of Coastal Sediments'87, ASCE, 884-900 pp.

Stwart, R., Ribas, F., Ruessink, G., Simarro, G., Guillén, J. (2017). Characteristics and dynamics of crescentic bar events in an open, tideless beach. Proceedings of the Coastal Dynamics 2017, Helsingør, Denmark, Paper no. 192, 12 p.

Van Enckevort, I.M.J. and Ruessink, B.G. (2003). Video observations of nearshore bar behavior. Part 1: alongshore uniform variability. Continental Shelf Research 23, 501–512. doi:10.1016/S0278-4343(02)00234-0.

van der Zanden, J., van der A, D. A., Hurther, D., Cáceres, I., O'Donoghue, T., Hulscher, S. J. M. H., & Ribberink, J. S., (2017a). Bedload and suspended load contributions to breaker bar morphodynamics. Coastal Engineering, 129, pp. 74-92.

van der Zanden, J., van der A, D.A., Hurther, D., Cáceres, I., O'Donoghue, T., Ribberink, J.S., (2017b). Suspended sediment transport around a large-scale laboratory breaker bar. Coastal Engineering, 125, pp. 51-69.

van der Zanden, Joep, Cáceres, I., Eichentopf, S., Ribberink, J. S., van der Werf, J. J., & Alsina, J. M., (2019). Sand transport processes and bed level changes induced by two alternating laboratory swash events. Coastal Engineering, 152, 103519.

Walstra, D.J.R., Reniers, A.J.H.M., Ranasinghe, R., Roelvink, J.A., Ruessink, B.G., (2012). On bar growth and decay during inter-annual net offshore migration. Coastal Engineering, 60, 190–200.

Walstra, D.J.R., Ruessink, B.G., Reniers, A.J.H.M. and Ranasinghe, R. (2015). Process-based modeling of kilometer-scale alongshore sandbar variability. Earth Surface Processes and Landforms, 40, 995–1005.

Walstra, D.J.R., Wesselman, D.A., van der Deijl, E.C., Ruessink, B.G. (2016). On the intersite variability in inter-annual nearshore sandbar cycles. Journal of Marine Science and Engineering, 4(1), 15.

Wijnberg, K., Kroon, A. (2002). Barred beaches, Geomorphology Journal 48, 103-12o p.

Highlights:

- Simple model to predict long-term evolution (years to decades) of two-bar systems as well as the response of feeder mounds;
- Simulation of individual bar volumes exposed to incident waves following an equilibrium-forced approach;
- Short calculation times while keeping the model stability;
- Potential for merging with a shoreline evolution model.

Bárbara Marinho
University of Aveiro
Department of Civil Engineering
Campus Universitário de Santiago
3810-193 Aveiro
Portugal

Editors-in-Chief
Journal of Coastal Engineering

Dear Editor-in-Chief Iñigo J. Losada

Please, find enclosed our revised manuscript, “Cross-shore modelling of multiple nearshore bars at a decadal scale” by Marinho *et al.*, which we would like to re-submit for consideration of publication as a Research Article in the International Journal of Coastal Engineering.

We appreciated all the received comments from the Journal to increase the value of the present paper. Based on these new inputs, we proceeded to our revision in order to accommodate the suggestions provided. A detailed description of our revision, as per the reviewers’ comments, is presented in the following pages. To make its presentation more efficient and intuitive, we organized the detailed description of changes in a table with two main columns: one corresponding to the received reviewer’s comments and other one with the description of our revision.

We confirm that this manuscript has not been published elsewhere and is not under consideration by another journal. All authors have approved the manuscript and agree with its resubmission to the International Journal of Coastal Engineering.

I am the corresponding author for this paper.

We look forward to hearing from you at your earliest convenience.

Sincerely,

Bárbara Marinho

Declaration of interests

☒ The authors declare that they have no known competing financial interests or personal relationships that could have appeared to influence the work reported in this paper.

☐The authors declare the following financial interests/personal relationships which may be considered as potential competing interests: